Analyst

Accepted Manuscript

ROYAL SOCIETY OF CHEMISTRY

www.rsc.org/analyst

Analyst

Dynamic Article Links ►

Cite this: DOI: 10.1039/c0xx00000x

www.rsc.org/xxxxxx

PAPER

A native chromatin extraction method based on salicylic acid coated magnetic nanoparticles and characterization of chromatin

Zhongwu Zhou[a] and Joseph Irudayaraj[*a, b]

Received (in XXX, XXX) Xth XXXXXXXXX 20XX, Accepted Xth XXXXXXXXX 20XX

DOI: 10.1039/b000000x

Native chromatin contains valuable genetic, epigenetic and structural information. Though DNA and nucleosome structures are well defined, less is known about the higher-order chromatin structure. Traditional chromatin extraction methods involve fixation, fragmentation and centrifugation, which might distort the higher-order structural information of native chromatin. We present a simple approach to isolate native chromatin from cultured mammalian cells using salicylic acid coated magnetic nanoparticles (SAMNPs). Chromatin is magnetically separated from cell lysates without any filtration or high-speed centrifugation. The purified chromatin is suitable for the examination of histone modifications and other chromatin associated proteins as confirmed by Western blotting analysis. Chromatin structure was determined by confocal fluorescence microscopy, transmission electron microscopy (TEM) and atomic force microscopy (AFM). High-resolution AFM and TEM images clearly show a classical bead-on-a-string structure. Higher-order chromatin structure is also determined via electron microscopies. Our method provides a simple, inexpensive and an environmental-friendly means to extract native chromatin not possible before, suitable for both biochemical and structural analysis.

Introduction

The structure of DNA [1] and nucleosome [2] are now well defined, and the basic 10-nm bead-on-a-string structure of chromatin is also discovered.[3] However, remarkably less is known about the higher-order chromatin structure and subsequent mechanisms for the organization of the chromatin fiber. Cryo electron microscopy study of reconstituted 30-nm chromatin fiber reveals a double helix twisted by tetranucleosomal units,[4] but scientists call into question the *in situ* evidence for the 30-nm fiber.[5] More specifically our knowledge of higher-order chromatin structure beyond 30 nm is limited, posing a constraint on our understanding of chromatin organization in the nucleus, selective gene expression, nucleosome passage during DNA replication and epigenetic control of gene expression etc. Resolving the chromatin structure, especially that of the interphase chromatin will open the doors to understanding its effect on DNA compaction, replication, transcription and repair.

Chromatin structure studies need better native chromatin sample preparation strategies so that structure can be better elucidated. Reconstituted chromatin *in vitro* do not represent the state of the native chromatin present in the nucleus since we neither know the level of cations in the nuclei nor be able to mimic the elegant and intricate conditions in the nucleus. Cryo sections of vitrified nuclei could be an intermediate step to obtaining the native material, however, the high level of non-chromatin components (salts and small organic molecules) in the nucleus with the almost same electron scattering power of chromatin can lead to very low resolution contrast images in which neither individual nucleosomes nor arrarys of nucleosome can be recognized.[6] There are obvious advantages for studying higher-order chromatin structures *in vitro*.[7] However, besides the time/labor involvement and the production of large amounts of toxic organic wastes, most of the present chromatin extraction methods cannot preserve the native chromatin structure.[8-12] The formaldehyde fixation process results in the cross-linking of proteins and these and other components contribute to impurities in the extraction, ascertained by mass spectrometry.[13, 14] Further, in the conventional methods, chromatin is sheared into shorter fragments via either nuclease digestion or sonication to separate them from cell debris via centrifugation;[15, 16] the heavy and large chromatin fibers containing higher-order structures are precipitated and discarded with the cell debris.

We apply the concept of solid-phase reversible immobilization (SPRI) and the non-specific binding between magnetic nanoparticles (MNPs) and polymer-like macromolecules to extract native chromatin. Without paraformaldehyde fixation, chromatin are directly magnetically isolated from cell lysates. The intact chromatin fiber is preserved without any fragmentation process, making it possible to observe higher-order structures by electron microscopy (EM). The extracted chromatin is suitable for further analysis such as the identification of histone modifications as well as chromatin associated proteins (ChAPs) via Western blotting (WB) analysis. The structure of chromatin extracted was also characterized by AFM and TEM.

Methods

Cell sample preparation

Non-neoplastic S1 HMT-3522 human mammary epithelial cells (HMEC), between passages 56 and 60, were plated at 2.3 X 10^4 cells/cm^2 for propagation as monolayers on plastic in chemically defined H14 medium.[17] When the cells were approximately 80%

confluent after maintaining for 7-10 days, they were harvested by treatment with trypsin and diluted in 10 ml DMEM/F12 medium (Invitrogen, 11965-118). 180 µl of soybean trypsin inhibitor (SBTI) was added to stop the trypsin (0.05%) digestion. The cell concentration was adjusted to approximately 1.0×10^6 cells/ml.

Preparation of salicylic acid coated magnetic nanoparticles

Water-dispersible salicylic acid coated magnetic nanoparticles (SAMNPs) were synthesized by previously reported method.[18, 19] Briefly, a 2:1:4 molar ratio of Fe (III): Fe (II): SA (salicylic acid) was added to a sterilized three-neck bottle containing NaOH solution (pH 11.0) with vigorous stirring with Ar gas. After refluxing at 90 ^{o}C for 4 h, a dark brown suspension was formed. The magnetic nanoparticles in the suspension were collected by magnetic separation and further washed to neutral pH with distilled water. The SAMNPs were dispersed in distilled water at a concentration of 10 mg/ml.

Extraction of chromatin by SAMNPs

Chromatin was purified from mammalian cells as follows. Typically, ~10^6 cells were collected in an Eppendorf tube by centrifugation (1000g, 5 min), then lysed by the addition of 100-µl lysis buffer (250 mM SDS, 1 mM EDTA, 0.5 mM EGTA, 1 mM PMSF and 2% Protease Inhibitor Cocktail (New England Biolabs)). The cell pellet was pipetted up and down slowly 20 times with a 200-µl pipette tip. 8-10 µl SAMNPs were added to form a chromatin-SAMNP complex and incubated for 10 min. 100 µl of isopropanol was added to the suspension and incubated for another 10 min at room temperature. After magnetic separation of the chromatin-SAMNP complex, the supernatant was discarded and the immobilized chromatin was rinsed once with 200 µl of ice cold 70% ethanol. After removal and evaporation of ethanol, chromatin was eluted in 50-100 µl of 1X phosphate buffered saline buffer (PBS) at RT for at least 1h. A further magnetic separation step was performed to obtain the released chromatin in the supernatant. The purified chromatin was then used for Western blotting (WB) and imaging analysis.

Western blotting analysis

The extracted chromatin was mixed with a 6X loading buffer (0.375M Tris pH 6.8, 12% SDS, 60% glycerol, 0.6M DTT, 0.06% bromophenol blue) and incubated at 37 ^{o}C for 20 min, then separated by electrophoresis through SDS-PAGE gels (crosslinking indicated in figure legends) and transferred to polyvinylidene fluoride membranes. The membranes were blocked with 5% milk to minimize non-specific antibody binding and then probed with specific primary antibodies histone 4, histone H3 trimethyl Lys27 (H3K27me3), nuclear matrix protein Lamin B and nuclear mitotic apparatus protein (NuMA). Supplementary Table 1 contains detailed antibody information. All antibodies were diluted in the blocking buffer and incubated overnight at 4°C in a wet chamber. The corresponding HRP-conjugated secondary antibodies were incubated with membranes at RT for 45 min. The membrane was developed in ECL buffer. Protein bands were visualized immediately after development using Western Lightning Plus-Enhanced Chemiluminescence Substrate (Perkin Elmer Life & Analytical Science).

Confocal microscopy analysis

50 µl of extracted chromatin was incubated with rabbit anti-human Histone 3 antibody at RT for 30 min, and washed 2 times with 1X PBS, then Alexa 647 conjugated goat-anti-rabbit IgG and Hoechst 34580 were added and incubated further for 45 min. The pellet was collected by centrifugation and washed 3 times with 1X PBS. The final product was dissolved in PBS and mounted on a glass cover slip. Directed staining by Hoechst 34580 was also performed in a similar manner. Fluorescence of Hoechst 34580 (excitation 405 nm, emission 461 nm) and Alexa 647 (excitation 650 nm, emission 668 nm) were detected using an inverted Zeiss LSM 710 (Carl Zeiss Microscopy Ltd, Cambridge) system and confocal images were collected using Zeiss LSM software (Carl Zeiss Microscopy Ltd, Cambridge).

AFM imaging

A drop of 5 µl chromatin solution was spotted onto a freshly cleaved mica surface (Ted Pella, Inc.) and incubated for 10s to allow chromatin to absorb onto the substrate. The sample drop was then washed off with 30 µL water, and dried with compressed air. Chromatin samples were imaged in air in the tapping mode on a Multimode AFM with Nanoscope IIIa controller (Veeco) using oxide-sharpened silicon probes with a resonance frequency in the range of 280-340 kHz (MikroMasch-NSC15). The tip-surface interaction was minimized by optimizing the scan set-point to the highest possible value. AFM imaging was performed at 25 °C. The images in TIFF format were prepared by NanoScope Analysis software.

TEM imaging

A 10 µl drop of purified chromatin was placed on a copper grid coated with carbon. After 30 s the grid was air dried and then negatively stained with 2% uranyl acetate for 2 min. The grid was then air dried and viewed in a Tecnai T20 microscope which is a 200KV transmission electron microscope with LaB6 filament.

Results and discussion

Advantages of magnetic separation

Magnetic nanoparticles are extensively applied for mechanical separation based on the fact that most biological systems do not have a naturally occurring magnetic component. When magnetic nanoparticles are applied as solid phase carriers forming MNPs-target molecule complexes, they can be selectively controlled in a magnetic field with high specificity and low background noise.[20] Long polymer-like macromolecules such as DNA tend to non-specifically wrap around nanoparticles and co-aggregate with the assistance of chaotropic agents such as PEG/NaCl or isopropanol.[21-23] They would induce DNA molecules transit from an elongated coil conformation to a very dense compact state, which is typically globular in shape. [24] The bications or

polycations in lysates would mediate the electrostatic interaction between negatively charged magnetic nanoparticles and the available portion of the DNA globule surface phosphate groups, resulting in DNA attachment onto the magnetic nanoparticle surface.

These nanoparticles reversibly release long polymer-like macromolecules in low salt solution. For example, DNA-MNP complexes disassociate from each other in TE buffer (pH 8.0). This is the basis for the solid-phase reversible immobilization (SPRI) introduced by Hawkins and coworkers.[25, 26] In a similar manner, we extract chromatin from cell lysates using salicylic acid coated magnetic nanoparticles (SAMNPs). The SAMNPs are well characterized in our previous work: 1) they are 10 nm in size as confirmed by TEM imaging; 2) they have a hydrodynamic diameter of approximately 122.7 nm with zeta potential at -38.1 mV in water.[19] The chemisorptions of salicylic acid onto Fe_3O_4 nanoparticle is through the oxygen group of carboxylic acid, which is symmetrically bonded to the Fe_3O_4 nanoparticle surface.[18]

When using SAMNPs for chromatin extraction, we expect the released chromatin in the lysates to be soluble; otherwise it will precipitate before attaching to the magnetic nanoparticle surface resulting in low yield. Previous studies applied 7.2% SDS to make chromatin soluble and determined that more than 1500 groups of nucleic acid associated proteins can be extracted and identified by mass spectroscopy.[14] We further confirmed that compared to chromatin extracted from 50 μL of 7.2% SDS, 500 μl of 0.72% SDS lysing buffer dos not result in significant differences in the thickness of the extracted chromatin fibers (noted in the Supplementary Fig.1). However, significant differences could be noted between extracted DNA and chromatin (Supplementary Fig.1). In our extraction process we use isopropanol instead of PEG/NaCl due to the high viscosity of the chromatin lysates. High concentration of PEG causes increased viscosity of the solution and prolonged magnetic separation process.

It is expected that the ionic milieu of the extraction reagents would affect chromatin structure, yet the nuclei levels of cations and polyamines are not known with certainty.[27-30] In order to mimic the physiological conditions and to reduce the structural variation of the extracted chromatin from different cell samples, we eluted chromatin from SAMNPs using 1X PBS buffer (137 mM NaCl, 2.7 mM KCl, 10 mM Na_2HPO_4 and 2 mM KH_2PO_4, pH 7.4). Because of the high ionic strength of PBS, the elution process was prolonged. Normally, it takes ~15 min (at RT) to elute DNA from SAMNPs in TE buffer, while it takes at least 1 h to obtain a similar concentration of chromatin in 1X PBS. Overnight elution at 4 ℃ could obtain a highly concentrated chromatin solution. If high yield is desired, it is more efficient to elute two or three times. Using 1X PBS as blank, chromatin absorbance from 1 million cells was determined at OD260 to indicate a 10 μg of DNA. The absorption spectra of extracted chromatin and corresponding DNA are also provided (Supplementary Fig. 2). Compared to the yield of commercial kits (4 μg/10^6 cells), the yield of our method (10 μg/10^6 cells) is 2.5 times higher and does not use any harsh reagents and considerably rapid.

Another advantage of the developed method is that cells are free of covalent crosslinking by formaldehyde or glutaraldehyde fixation. Though these aldehyde-based fixatives enable strong crosslinking and fixation of proteins, they may give rise to possible artifacts such as the denaturation of epitopes for antibody staining and change in protein conformation.[13, 14] Compared to the cross-linked chromatin product, chromatin extracted by the SAMNP technique is native, and provides single-nucleosome-level resolution and avoids non-specific modification signals from different nucleosomes carried over through protein-protein interactions.[31]

Identification of chromatin associated proteins

Since the extracted native chromatin contains both chromatin associated proteins (ChAPs) and DNA, they can be used for the identification of ChAPs. Western blotting (WB) was used to examine ChAPs, both the histone proteins and non-histone proteins. The protein bands corresponding to trimethylation of histone H3 lysine 27 (H3K27me3, 15.3 kD) and histone 4 (H4, 11.3 kD) can be clearly noted in Fig. 1(B). Two other non-histone proteins, nuclear mitotic apparatus protein (NuMA, 240kD) and nuclear matrix protein Lamin B (66kD), were also detected as shown in Fig. 1(C). We were not able to detect splicing regulator SC35 by WB (data not shown), which is consistent with recent reports that this protein is absent in ChAP preparation [14]. To investigate the sensitivity of the chromatin preparation method, chromatin was extracted from different numbers of cells (1, 2 and 3 million), as expected, the intensity of H3K27me3 and H4 increased. (Fig. 1(B)). We also examined the ChAPs by SDS-PAGE, stained by Coomassie blue and presented in the supplementary Fig. 3. The successful identification of histones with the right size by WB confirmed that histone proteins exist in the extracted chromatin product. The identification of H3K27me3 in the extracted chromatin implied that this specific epitope of the modified histone was not masked by the high concentration of SDS. Negative control experiments for SC35 protein, a nuclear protein with Western blotting analysis provides good evidence of high quality data. However, extensive experiments need to be conducted, including, possibly proteomic studies to confirm the proteins and other impurities that could to the chromatin. IT is our expectation that purifications steps can commence depending upon the level of purity expected from the extracted sample.

The extracted chromatin was also stained with Hoechst 34580, a blue fluorescent dye specific for nucleic acids, and analyzed by confocal microscopy, as shown in Fig.2. The yield of extracted chromatin was very high as noted in Fig.2A. Because of the relatively low resolution of light microscopy, most of the extracted chromatin appeared rod-like, and its detailed structure could not be observed. Double staining studies were also performed on the extracted chromatin. Samples were stained first with Alexa 647-labeled anti-rabbit secondary antibody against Histone 3 primary antibody, and then with Hoechst 34580 against DNA, and examined by confocal microscopy, as showed in Fig.2 (C~H). Histone and DNA are the primary components of chromatin, thus the successful double staining confirmed that the extracted material is chromatin. We conclude that the chromatin extracted by our approach is in the heterochromatin form, a tightly packed form of DNA in the whole chromatin. We also

observed the extracted chromatin by dark-field microscopy (supplementary Fig. 4) from their innate scattering signals.

Characterization by confocal fluorescence microscopy which has a resolution of approximately 200~400 nm, revealed only larger fibers (hundreds nanometers) or only highly condensed metaphase chromosomes. To observe higher-order structures of chromatin, most of the past work focused on EM studies. Scanning probe microscopy, especially AFM, has significant advantages but has a lower resolution. Imaging in air at ambient humidity, native chromatin remained unstained and hydrated. Chromatin fibers at different levels (from 10 nm to 500 nm) were observed in Fig.3A. Fig. 3C showed chromatin structure at single nucleosome resolution. And a clear bead-on-a-string structure was visible in Fig. 3D. Long 10-nm fibers were also observed (Supplementary Fig.5). Many bright spots were found in the background, which might be from the stropped proteins during storage. These stropped proteins can be reduced by post-fixation; however, in order to not affect chromatin structure, post-fixation was avoided.

Characterization of chromatin via electron microscopies

Numerous studies have been reported on chromatin structure, either from the nuclear cross sections which provide general but blurred chromatin images or from the extracted chromatin examined by electron microscopy which provides a clear bead-on-a-string structure. However, a challenge is on how to integrate the two types of information.[6, 32] Cryo sections of vitrified nuclei could provide intermediately resolved images that reduce the gap between the molecular and cellular scales. However, the high level of non-chromatin components (salts and small organic molecules) in the nucleus with almost the same electron scattering power of chromatin can lead to very low resolution contrast images in which neither individual nucleosomes nor arrays of nucleosome can be recognized from the EM images.[6] AFM characterization of purified native chromatin might bridge the resolution gap by providing both the general and detailed structure images.

Combining our native chromatin extraction method with high resolution AFM characterization, we provide a general view of the interphase chromatin, as shown in Fig. 3A~D. The images show chromatin fiber at different levels from 10 nm (Fig.3D) to 500 nm (Fig. 3A). Fig. 3A clearly shows how the 10-nm fiber is organized into higher-order chromatin from 20~60 nm. These 60-nm fibers could possibly contribute to the the assembly of 300-nm fiber and even 500-nm fiber. We also found that the 10-nm fiber may occasionally contribute to the assembly of ~ 30-nm fiber. This is also consistent with the data obtained from TEM images.

DNA replication is a semi-conservative process of producing two identical copies an original DNA molecule, which occurs in all living organisms. In eukaryotic cells, in order to maintain identity within cell lineages, the epigenome as well as the genome needs to be faithfully replicated in each cell cycle, including DNA modifications, histone modifications and nucleosome positioning. After nascent DNA strands form behind the replication fork, they are rapidly reorganized into nucleosomes. The 'old' parental histones in coordination with the assembly of the newly synthesized histones are transferred to form histone octamers on the nascent DNA strands,[33] which also are known as parental histone segregation and replication-dependent *de novo* nucleosome assembly, respectively.[34] It is not yet known how these two processes are coordinated to preserve genetic stability in terms of nucleosome positioning. We addressed this issue by images of the replication fork. Each replication fork is defined by two bifurcations of the chromatin stand, producing a "bubble-like" configuration,[35] as shown in Fig. 4. Each strand of the replication fork was around 10 nm, which is the lowest level of chromatin fiber. From these images, it is easy to note that the nucleosomes are not evenly distributed on the two nascent strands of the replication fork. This could be due to the fact that the parent H3-H4 tetramers may not be equally split into H3-H4 dimers in the two nascent strands. Further studies are necessary to address this question.

Chromatin conformation capture (3C) assays and related technologies (5C and HiC) have been used to identify physical interactions among chromatin elements in a genome-wide fashion. However, important features of genome organization and function can't be measured by these technologies, such as the higher-order chromatin organization and dynamics at the chromosomal level, or genome-wide determination of functional interactions between genomic DNA and its regulators. Fig 3A and 3B shows that, even in one single chromatin, several chromatin fibers exist and interact with one another. Two interesting structures are shown in Fig.5. In each image, two nucleosomes, indicated by black arrows may merge the two separate DNA strands together. This type of structure is not likely derived from the replication fork, and their function is still unknown.

Fig. 6 shows TEM micrographs of the extracted chromatin at different scales from 10 nm to 200 nm. The chromatin was stained with uranyl acetate (2%), and as expected, heterochromatin was observed at the compact regions of chromatin denoted by red arrows (Fig 4A-F). Most of the extracted chromatin was highly condensed, which is consistent with our confocal microscopy data. The complex structure of chromatin makes it hard to measure the length of whole chromatin (scale bar is provided). Interestingly, in some micrographs (Fig. 4 A-D), the terminal end of chromatin was heavily protected by the formation of a T-shaped structure. This may help to explain how cells keep chromatin from fusing, consistent with the past findings.[36] The classical bead-on-a-string structure were also observed at high magnification (Fig. 4 G~I), which is consistent with our AFM characterization. Images show that the chromatin structure was most likely preserved and we could observe the chromatin fiber at different scales from 10-800 nm, possibly at different levels of organization. These TEM images (Fig.4) provide a better understanding of chromatin organization inside the compacted nucleus, which could not be seen by other conventional approaches that often use thin slices or sections.[37]

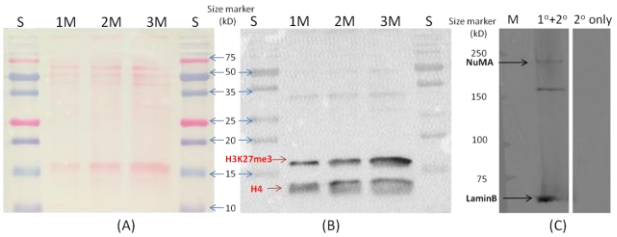

Figure 1. Western blotting of ChAPs. Chromatin extracted from different amounts of cells (~ 1, 2 and 3 , M= million, respectively), and loaded on a 15% SDS-PAGE, transferred to membrane and further stained by Ponceau S solution (A), blocked, and then incubated with H3K27me3 and H4 antibodies. The membrane was developed two times to obtain the two bands (B). Chromatin from ~ 10^6 cells were extracted, and loaded on a 5% SDS-PAGE, and incubated with NuMA and Lamin B antibodies. The band could only be detected with both the primary (1°) and the corresponding secondary (2°) antibodies. The negative control (2° only) did not show the presence of any bands (C).

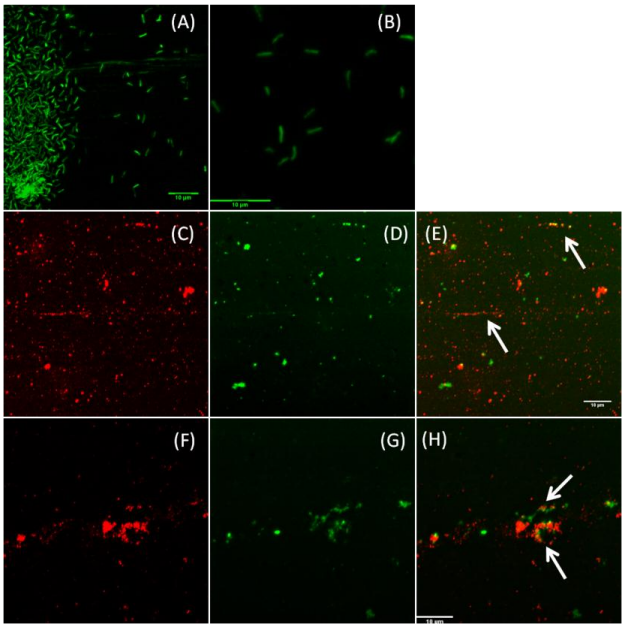

Figure 2. Hoechst 34580 stained chromatin visualized by confocal microscopy (A, B). Double immunostaining of extracted chromatin (C~H). H3 was stained with Alexa 647 (red, C and F), and DNA was stained by Hoechst 34580 (green, D and G) for immunofluorescence experiments. ImageJ was used to obtain the merged images (E and H). The white arrows indicated the stained chromatin. Scale bar, 10 µm.

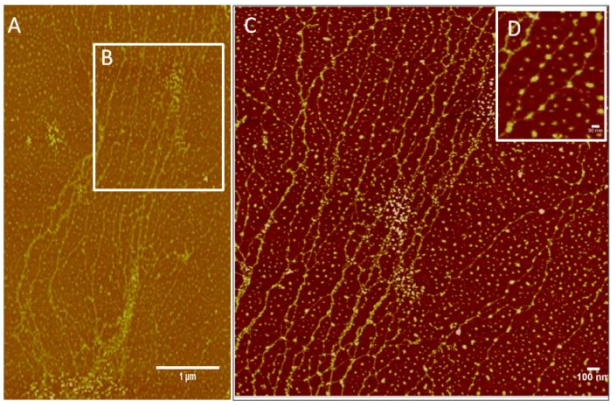

Figure 3. AFM images of extracted chromatin. Images were obtained in air at ambient humidity. Large scale scanning was performed (A), chromatin fiber at different levels (from 10 ~ 300 nm) was observed. A detailed part of (B) (the white square) was rescanned in (C), the typical 10 nm, "bead-on-a-string" structure was clearly observed, and these fibers crosslink to one another to form larger fibers (about 20 nm). An enlarged part of C was given in D, and a replication fork-like structure was observed. Single nucleosome could be clearly observed. Scale bar are provided in the lower right of each figure by ImageJ.

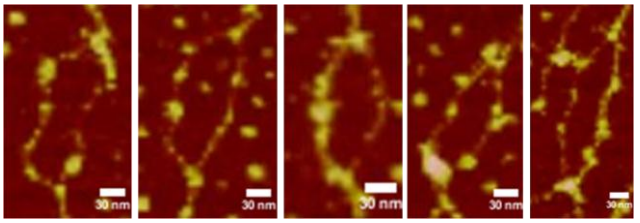

Figure 4. Non-evenly distributed nucleosomes on the two nascent DNA strands.

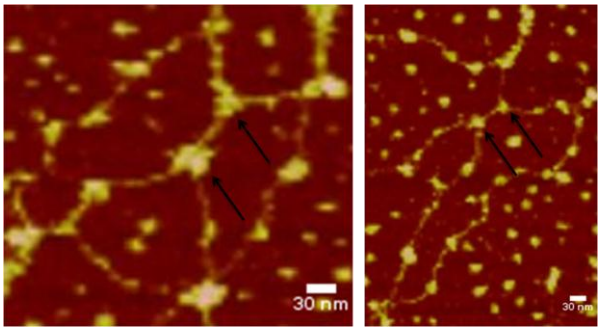

Figure 5. Complex chromatin structure. The black arrow indicates the nucleosome and/or ChAPs which merge the two separate DNA strands together.

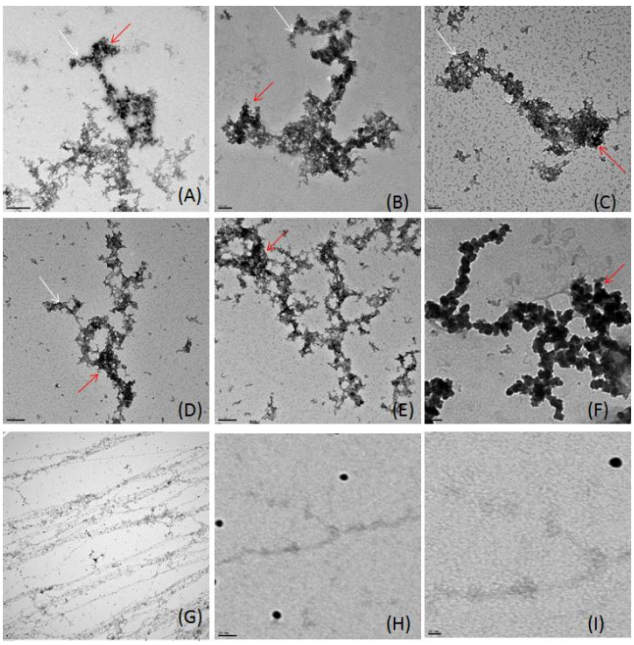

Figure 6. TEM image of extracted chromatin. The white arrows indicated a T shape structure, which may help to explain how cells keep chromatin from fusing. The red arrows indicated heterochroamtin at compact regions of chromatin. The scale bars from A to I were 500 nm, 100 nm, 100 nm, 200 nm, 200 nm, 100 nm, 2000 nm, 50 nm and 20 nm, respectively.

Conclusions

In summary, we have demonstrated an elegant and rapid methodology to extract native chromatin from mammalian cells based on salicylic acid coated magnetic nanoparticles. The extracted native chromatin contains valuable genomic, epigenetic and structural information, which can serve as the basis for biochemical and biophysical analysis. Western blotting analysis was used to identify both epigenetic marks and chromatin associated proteins to confirm the authenticity of the extracted fibers. The extracted chromatin can be used for the identification of chromatin associated proteome via mass spectroscopy. Double immunofluorescence staining confirmed the presence of both the DNA and histone components on the extracted chromatin allowing an opportunity to explore DNA and histone modification patterns with high-resolution. High-resolution AFM images show a clear bead on a string structure and other fine structures at the single-nucleosome resolution level.

Acknowledgements

This project was partly funded by the W.M. Keck Foundation. Funding from the Indiana CTSI, the Purdue Center for Cancer Research (NIH-NCI funded) CORE grant and the NSF 1249315 grant. The authors thank Sophie Lelièvre and members of her laboratory for providing cell culture training and assistance in Western Blot analysis. We thank Jill Hutchcroft for proof reading and comments. Thanks to Arnold Stein and John Anderson for their insightful discussions. Zhi Shan, Pengfei Wang, Don Ready and Xiaolei Wang are acknowledged for technical assistance.

Notes and References

[a]*Bindley Bioscience Center and Birck Nanotechnology Center, Purdue University, West Lafayette, IN 47907, USA.; E-mail: zhou255@purdue.edu.*
[b]*Agricultural & Biological Engineering, Purdue University, 225 S. University Street, West Lafayette, IN 47907-2093, USA. Fax: 7654961115; Tel:7654940388; E-mail: josephi@purdue.edu*
† Electronic Supplementary Information (ESI) available: [details of any supplementary information available should be included here]. See DOI: 10.1039/b000000x/

1. Watson, J.; Crick, F. A structure for deoxyribose nucleic acid. *Nature* 1953, 421, 397-3988.
2. Luger, K.; Mader, A. W.; Richmond, R. K.; Sargent, D. F.; Richmond, T. J. Crystal structure of the nucleosome core particle at 2.8A resolution. *Nature* 1997, 389, 251-260.
3. Woodcock, C. L.; Horowitz, R. A. Chromatin organization re-viewed. *Trends Cell Biol* 1995, 5, 272-7.
4. Song, F.; Chen, P.; Sun, D.; Wang, M.; Dong, L.; Liang, D.; Xu, R.-M.; Zhu, P.; Li, G. Cryo-EM Study of the Chromatin Fiber Reveals a Double Helix Twisted by Tetranucleosomal Units. *Science* 2014, 344, 376-380.
5. Eltsov, M.; MacLellan, K. M.; Maeshima, K.; Frangakis, A. S.; Dubochet, J. Analysis of cryo-electron microscopy images does not support the existence of 30-nm chromatin fibers in mitotic chromosomes in situ. *P Natl Acad Sci USA* 2008, 105, 19732-19737.
6. Horowitz-Scherer, R. A.; Woodcock, C. L. Organization of interphase chromatin. *Chromosoma* 2006, 115, 1-14.
7. Giannasca, P. J.; Horowitz, R. A.; Woodcock, C. L. Transitions between in situ and isolated chromatin. *J Cell Sci* 1993, 105 (Pt 2), 551-61.
8. Bhorjee, J. S.; Pederson, T. Chromatin. Its isolation from cultured mammalian cells with particular reference to contamination by nuclear ribonucleoprotein particles. *Biochemistry* 1973, 12, 2766-2773.
9. Harlow, R.; Wells, J. Preparation of membrane-free chromatin bodies from avian erythroid cells and analysis of chromatin acidic proteins. *Biochemistry* 1975, 14, 2665-2674.
10. Monahan, J. J.; Hall, R. H. Preparation of chromatin from tissue culture cells—A convenient method. *Anal.Biochem.* 1975, 65, 187-203.
11. Pederson, T. Isolation and characterization of chromatin from the cellular slime mold, Dictyostelium discoideum. *Biochemistry* 1977, 16, 2771-2777.
12. Kornberg, R. D.; Lapointe, J. W.; Lorch, Y. [1] Preparation of nucleosomes and chromatin. In *Methods in Enzymology*, Paul, M. W.; Roger, D. K., Eds. Academic Press: 1989; Vol. Volume 170, pp 3-14.
13. Jiang, X.; Jiang, X.; Feng, S.; Tian, R.; Ye, M.; Zou, H. Development of Efficient Protein Extraction Methods for Shotgun Proteome Analysis of Formalin-Fixed Tissues. *J Proteome Res* 2007, 6, 1038-1047.
14. Zhang, Y.; Hu, Z.; Qin, H.; Wei, X.; Cheng, K.; Liu, F.; Wu, R. a.; Zou, H. Highly Efficient Extraction of Cellular Nucleic Acid Associated Proteins in Vitro with Magnetic Oxidized Carbon Nanotubes. *Anal Chem* 2012, 84, 10454-10462.
15. Bhorjee, J. S.; Adler, L. Nuclear shearing and chromatin structure. *Cell Biol Int Rep* 1982, 6, 1065-1076.
16. Woodcock, C. L.; Sweetman, H. E.; Frado, L. L. Structural repeating units in chromatin. II. Their isolation and partial characterization. *Exp Cell Res* 1976, 97, 111-9.
17. Abad, P. C.; Lewis, J.; Mian, I. S.; Knowles, D. W.; Sturgis, J.; Badve, S.; Xie, J.; Lelièvre, S. A. NuMA influences higher order chromatin organization in human mammary epithelium. *Mol Bio Cell* 2007, 18, 348-361.
18. Unal, B.; Durmus, Z.; Kavas, H.; Baykal, A.; Toprak, M. S. Synthesis, conductivity and dielectric characterization of salicylic acid–Fe3O4 nanocomposite. *Materials Chemistry and Physics Mater Chem Phys* 2010, 123, 184-190.

19. Zhou, Z.; Kadam, U. S.; Irudayaraj, J. One-stop genomic DNA extraction by salicylic acid-coated magnetic nanoparticles. *Anal Biochem* 2013, 442, 249-252.
20. Beveridge, J. S.; Stephens, J. R.; Williams, M. E. The use of magnetic nanoparticles in analytical chemistry. *Annu Rev Anal Chem*2011, 4, 251-273.
21. Shan, Z.; Wu, Q.; Wang, X.; Zhou, Z.; Oakes, K. D.; Zhang, X.; Huang, Q.; Yang, W. Bacteria capture, lysate clearance, and plasmid DNA extraction using pH-sensitive multifunctional magnetic nanoparticles. *Anal Biochem* 2010, 398, 120-122.
22. Shan, Z.; Zhou, Z.; Chen, H.; Zhang, Z.; Zhou, Y.; Wen, A.; Oakes, K. D.; Servos, M. R. PCR-ready human DNA extraction from urine samples using magnetic nanoparticles. *J Chromatogr B* 2012, 881, 63-68.
23. Zhou, Z.; Kadam, U. S.; Irudayaraj, J. One-stop genomic DNA extraction by salicylic acid-coated magnetic nanoparticles. *Anal Biochem* 2013, 442, 249-52.
24. Shan, Z.; Jiang, Y.; Guo, M.; Bennett, J. C.; Li, X.; Tian, H.; Oakes, K.; Zhang, X.; Zhou, Y.; Huang, Q.; Chen, H. Promoting DNA loading on magnetic nanoparticles using a DNA condensation strategy. *Colloids Surf., B*
25. Hawkins, T. L.; O'Connor-Morin, T.; Roy, A.; Santillan, C. DNA purification and isolation using a solid-phase. *Nucleic Acids Res* 1994, 22, 4543.
26. DeAngelis, M. M.; Wang, D. G.; Hawkins, T. L. Solid-phase reversible immobilization for the isolation of PCR products. *Nucleic Acids Res* 1995, 23, 4742-4743.
27. Woodcock, C. L.; Dimitrov, S. Higher-order structure of chromatin and chromosomes. *Curr Opin Genet Dev* 2001, 11, 130-5.
28. Bednar, J.; Horowitz, R. A.; Dubochet, J.; Woodcock, C. L. Chromatin conformation and salt-induced compaction: three-dimensional structural information from cryoelectron microscopy. *J Cell Biol* 1995, 131, 1365-76.
29. Bednar, J.; Horowitz, R. A.; Grigoryev, S. A.; Carruthers, L. M.; Hansen, J. C.; Koster, A. J.; Woodcock, C. L. Nucleosomes, linker DNA, and linker histone form a unique structural motif that directs the higher-order folding and compaction of chromatin. *P Natl Acad Sci U S A* 1998, 95, 14173-8.
30. Carruthers, L. M.; Bednar, J.; Woodcock, C. L.; Hansen, J. C. Linker histones stabilize the intrinsic salt-dependent folding of nucleosomal arrays: mechanistic ramifications for higher-order chromatin folding. *Biochemistry* 1998, 37, 14776-87.
31. Cuddapah, S.; Barski, A.; Cui, K.; Schones, D. E.; Wang, Z.; Wei, G.; Zhao, K. Native Chromatin Preparation and Illumina/Solexa Library Construction. *Cold Spring Harbor Protocols* 2009, 2009, pdb.prot5237.
32. Cardoso, M. C.; Schneider, K.; Martin, R. M.; Leonhardt, H. Structure, function and dynamics of nuclear subcompartments. *Curr Opin Cell Biol* 2012, 24, 79-85.
33. Lucchini, R.; Wellinger, R. E.; Sogo, J. M. Nucleosome positioning at the replication fork. *EMBO J* 2001, 20, 7294-7302.
34. Groth, A.; Rocha, W.; Verreault, A.; Almouzni, G. Chromatin Challenges during DNA Replication and Repair. *Cell* 2007, 128, 721-733.
35. McKnight, S. L.; Miller Jr, O. L. Electron microscopic analysis of chromatin replication in the cellular blastoderm drosophila melanogaster embryo. *Cell* 1977, 12, 795-804.
36. Nikitina, T.; Woodcock, C. L. Closed chromatin loops at the ends of chromosomes. *J Cell Biol* 2004, 166, 161-5.
37. Woodcock, C. L.; Ghosh, R. P. Chromatin higher-order structure and dynamics. *Cold Spring Harb Perspect Biol* 2010, 2, a000596.

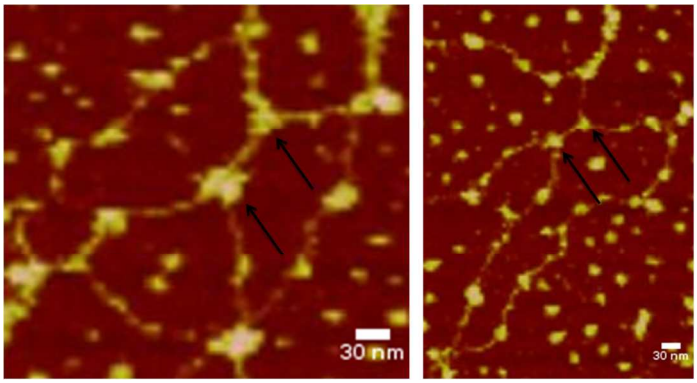

Native chromatin extraction with salicylic acid coated magnetic particles